

THE FAILURE OF THE ALTERNATORS OF THE NIMROD MAIN MAGNET POWER SUPPLY

H. G. Brooks  
Rutherford High Energy Laboratory, England

A. B. D. Reed  
English Electric Co., Ltd., England

Summary

The paper describes the failure of one of the two magnet power supply alternators which resulted in the rewind of one stator and the modification and rebuild of the rotors of both alternators. This failure prevented Nimrod operating at 7 GeV from late February, 1965 to the end of November, 1965. Certain design changes made when the rotors were rebuilt are described. A resumé is given of the investigations carried out immediately after the failure, while rebuilding was in progress, and after the machines were returned to service. Present plans are also briefly mentioned.

1.0 Description of Installation

Duty of Power Supply<sup>1</sup>

A power supply consisting of two 60 MVA 1,000 r/min motor-alternator-flywheel sets feeding transformers and mercury arc convertors is interposed between the magnet and the electricity supply network.

During the current rise period the machines act as generators, and at the beginning of flat top, half the convertors are switched from rectification to inversion, the remaining half following into inversion at the end of the flat top period. During decay time, energy is returned from the magnet to the machines which now operate as synchronous motors (Figs 1a and 1b). The pole construction as originally designed is shown in Fig 2.

2.0 The Failure

On the evening of February 21st, 1965, a loud thud was heard from No. 1 alternator and dense smoke emerged from it. The emergency trip was operated and the set came to rest under braking in 15 mins. The alternators were not energised at the time of the fault, and the alternator which failed had been subjected since it was commissioned to  $7.25 \times 10^6$  pulses. Pedestal vibration and shaft eccentricity readings were normal even seconds before the incident.

3.0 Investigation of Failure

3.1 Site examination of machine

The fault was caused by the fatigue failure of a rotor pole endplate across the neck region (Figs 3 & 4). Both drive motor rotors had rubbed on their stator laminations. All pedestals and the endplates of No. 2 alternator were examined for cracking and found to be sound.

It was therefore decided to carry out strain gauge measurements in the neck region. The stress distribution across the neck with the set

at no load speed was about 44,000 lbf/in<sup>2</sup> towards the neck edge and approx. 19,000 lbf/in<sup>2</sup> at the neck centre. It was noticed that superimposed on the D.C. stress due to CF force was an alternating gravitational component of stress at rotational frequency having an approximate value of 1,450 lbf/in<sup>2</sup>. At this stage the tests were prematurely discontinued because a very small crack was detected in an endplate.

3.2 Detailed examination of rotor

The rotor was very carefully dismantled and all details recorded. Four other endplates on the failed rotor were found to have cracks and only one failure was not at the flywheel end, where the large shaft torque changes occur. There was little evidence of a preferred side for the crack to start. This suggested that tensile and transverse bending stresses could be significant.

The pole side of the keys showed that laminated portions of the pole were well bedded against the key surface, with little sign of fretting or pick-up. In the region of the endplate there was evidence of fretting especially on the top edge of the key.

The rotor bodies were examined for cracking and were found to be sound. Laminations were found to be satisfactory except for those adjacent to endplates in which advanced cracks were present.

3.3 Theoretical Analysis

The dovetail fixing had been considered during the original design and photoelastic tests had indicated a stress concentration factor (S.C.F.) of 1.7. The reasons for failure were not readily apparent. Because of this two fields were investigated:

- (i) Additional forms of loading which could be significant.
- (ii) Examination of the known loadings to determine whether they acted in a different manner to that anticipated in the original design.

3.3.1 Additional loadings. Both rotors had been subjected to the effects of more rectifier backfires than anticipated but this was not considered to be a cause of failure. The effects of flux changes were reconsidered and the original design levels confirmed. The dynamics of the complex pole-shaft-flywheel system structure were analysed. It was found that the torque loads could be up to 20% higher on the flywheel end, but again this was not considered to be significant.

3.3.2 Alternative mechanisms for known loading. The main loads on the dovetail neck are

due to centrifugal force, torque and gravity.

The end turns were supported on a projecting lip on the endplate. In the original design it was considered that this eccentric load was resisted by the laminations and that the endplate was able to take up the appropriate attitude. However, if the dovetail is restrained and the support offered by the laminations small then considerable bending moments can be produced. Tests on the poles showed that such a mode of behaviour was possible even with normal consolidation. Stress variation due to speed is superimposed on the direct and bending components.

The effects of gravity on the pole stresses had been examined but the variable stress on the neck due to the self weight of the pole, was small. It however acts in a more subtle way. Due to the sag of the shaft there is a very small angle  $\epsilon$  (Fig. 5) between the catenary line at the endplate and the axis A B. This means that the effective pole length oscillates between C D and E F producing changes in lamination pressure and a resulting rotational frequency bending about the X X axis (Fig. 2). This stress variation is a feature of all horizontal machines of keyed laminated pole construction.

Reference to table 1 shows that without stress concentration it was estimated that the mean direct tensile stress across the neck was in the range 31-39,000 lbf/in<sup>2</sup> upon which was superimposed a variable component of 3,400-4,200 lbf/in<sup>2</sup>. Even after allowing for S.C.F. of 1.7 (based on the nominal neck stress) a Goodman diagram for the conditions shows the endplate to be well removed from failure.

It was clear that a fundamental discrepancy existed.

Interest became centred on the local conditions between the key and pole dovetail. The situation had features in common with failures of steam turbine shafts at low variable stresses.<sup>2</sup> These were:-

- (i) The key and pole are held in contact under high compressive stresses and could behave as solid material.
- (ii) In such a configuration as in (i) then the transition between dovetail neck and key represents a very sharp corner. Material in this corner is subject to high tensile stresses.

If strength reduction factors comparable with those found in the turbine investigation were applicable, failure could occur.

Some of the cracks in the endplates had propagated in the areas of fretting damage at the top corner of the key. The torsion of the shaft and the small changes of centrifugal loading could both produce the required oscillatory movement for fretting fatigue damage to occur. The necessary pressure is inherent in the arrangement. Further theoretical analysis of this aspect was difficult and experimental work was essential.

#### 4.0 Modified Design

It was essential to have the proton synchrotron operational again in the shortest possible time. A decision to radically redesign the rotors would have meant up to two years delay and so it was decided that provided worthwhile improvements could be made, the existing rotor forgings and pole laminations should be used again. With this policy it was clear that the basic keyed pole construction was implied. These decisions had to be made well before any of the extensive theoretical and laboratory investigations were completed, but there was sufficient confidence that a real improvement could be achieved, to justify this course of action.

The following modifications were made:-

- 4.1 The endplate material was changed to a high strength forging to give a gain of 50% to 60% in nominal properties. The forgings were arranged to obtain good grain flow in the critical neck region, and were heat-treated to develop a yield strength of 110,000 lbf/in<sup>2</sup>.
- 4.2 The neck thickness was increased from 5 ins to 6 ins to reduce neck stresses.
- 4.3 The dovetail geometry was modified by introducing a relief (Fig. 6) so that both fretting and stress concentration problems were reduced. Additionally the key was extended axially past the pole.
- 4.4 The machining processes on the endplate were arranged as far as possible for any machining marks to lie parallel to the neck axes, thus giving the best fatigue resistance. The stressed areas were finished by polishing to about 16 micro inch finish.
- 4.5 To minimise any bending stresses due to the overhung copper the laminations were consolidated during pole construction to three times the original pressure and retained by higher tensile tie rods.
- 4.6 Close attention was paid to the quality of the bedding between keys and pole, especially in the region of the endplate.
- 4.7 A phosphate/molybdenum disulphide treatment was applied to the keys to reduce the extent of fretting and corrosion and hence the risk of crack initiation.
- 4.8 The location of rotor excitation connections was altered in order to allow access to the endplates for ultrasonic examination.

#### 5.0 Experimental Investigations

##### 5.1 Laboratory Tests

The aims of the test programme were:-

- (i) To verify that the actual failures could be reproduced at appropriate loads.
- (ii) To investigate the effect of changes of dovetail geometry and material and hence assess the performance of a modified design.

A rig was designed to accept a full sized section of endplate but of reduced thickness. The actual loading in the rotor is a complex combination of pulsating direct loads, and bending stresses in two planes. Any attempt to reproduce this exactly would be impracticable. The loading system was therefore simplified to represent the cross section with the highest stress, i.e. the outer surface of the endplate. A steady tensile load was applied by a hydraulic jack, and the variable direct and bending stresses were produced by a rotating out-of-balance weight attached to the test specimen at an appropriate point. In addition to fatigue tests the rig was used for photoelastic coating investigations.

The first step was to attempt to reproduce the conditions of the failure. Tests were carried out at a mean nominal stress of 43,500 lbf/in<sup>2</sup>. The cyclic stress component was varied from 19,500 lbf/in<sup>2</sup> to 14,000 lbf/in<sup>2</sup> over 8 unrelieved cast endplate specimens and the results of these runs gave a stress-life curve and mode of failure (Fig. 7), which was acceptably consistent with the actual one.

Cast steel specimens with relief, and forged steel specimens with and without relief were prepared. A test programme along similar lines to the original was laid down for each and Fig. 7 shows the results obtained. It was found the fatigue limit was equivalent to 29,000 lbf/in<sup>2</sup> for the new endplates compared with about 14,500 lbf/in<sup>2</sup> for the original endplates, both at the same steady stress level.

With this vindication of the redesign tests were continued to ensure that no mechanism (such as fretting) would become significant after a large number of cycles. Two test runs were successfully extended to 10<sup>8</sup> cycles at stresses above operating conditions.

## 5.2 Site Testing

5.2.1 Strain gauge measurements. Strain gauge measurements using resistance wire gauges showed steady stress levels to be generally as predicted (Table 1) but alternating stresses when pulsing could not be accurately assessed because of high noise level due primarily to the gauge locations within the machine. It was possible that fast stress overshoots might occur particularly at torque change periods due, for example, to pole mechanical resonance effects.

Piezo electric strain gauges were used even though it was realised that very small outputs would be obtained at pulsing frequency. However the gravitational component of stress, to which reference has already been made, was clearly observed and this suggested that any rapid stress changes should have been apparent. No such excess stress levels were observed.

Silicon piezo resistive strain gauges having strain sensitivities almost one hundred times greater than conventional resistance wire gauges were finally used. These proved very satisfactory for cyclic stress measurements and confirmed estimated stress figures. Again no excess stress

overshoots were observed.

In all the foregoing measurement systems an excellent response could be expected at all frequencies up to 900 cycles per second.

## 5.3 Site photoelastic investigation<sup>3</sup>

### 5.3.1 Work carried out on experimental rigs.

Investigation using a test rig similar to that described in Section 5.1 confirmed that the S.C.F. across the neck section was about 1.7 but in the 5/8 in radiused neck edge region it was found to be 1.9 ±0.2 for the new design and 2.15 ±0.2 for the old design.

It was also found that on the new design the very localised region of maximum tensile stress occurred about 2/3 of the way round the 5/8 in radius away from the key, whereas in the old design the distance of the highest tensile stress was only about half this distance away from the key.

### 5.3.2 Work carried out on an alternator pole endplate under operational conditions

Photoelastic material was cemented to a pole endplate and techniques were developed to enable still and cine photography to be carried out when the machine was pulsing. The highest stress observed in the neck region immediately above the thick key section was 55,000 lbf/in<sup>2</sup> ±6,700 lbf/in<sup>2</sup>. Only 41,500 lbf/in<sup>2</sup> ±4,500 lbf/in<sup>2</sup> was observed just above the thin key section. It was not easy to evaluate the cyclic stress components since they represented only about 0.3 of a colour fringe. With a S.C.F. of 2 applied it will be noted that these figures are in close agreement with Table 1.

Compressive stresses in the pole endplate immediately adjacent to the thick key region were observed to be of the order of 72,000 lbf/in<sup>2</sup>.

## 5.4 Measurement of relative movement between key and endplate

A transducer was used to measure the displacement between key and endplate. As the machine ran up to speed a movement of 0.004 in occurred and when pulsing further movements up to 0.0003 in were recorded. It is frequently held that the most serious fretting attacks which tend to lead to cracking occur when the relative displacements of the two surfaces in question are 0.0002 in to 0.002 in.

## 6.0 Analysis of Probable Causes of Failure

Investigation results show that in the original design, crack initiation could occur due to either fretting or conventional fatigue, the stresses necessary to cause this being of similar order of magnitude. The reduction of the fretting phenomena by having a relieved profile on the cast specimens produced little improvement. The unrelieved forged specimens failed by fretting-fatigue. Once any crack is formed the higher mechanical strength of this material was not fully realised because of notch sensitivity. With the removal of the fretting situation to a "safer" area by provision of the relief, the improved

properties of the forging were now utilised, and additionally the strength reduction factor was lower than that of the casting. With the reduction of stresses in the new design and the improved strength of the arrangement it is estimated that on the basis of variable load levels the design is improved by a factor approaching 10.

It is concluded that the failure was due to a combination of three factors, each of which acting alone would not have produced failure. These factors were:-

- (i) The precise mechanism by which the stress summation at certain critical points was aggravated by the pulsing duty was not fully appreciated.
- (ii) The geometry and material were such that a high strength reduction factor was obtained.
- (iii) Fretting occurred in a critical region.

7.0 Present Policy

The rebuilt rotors have now been subjected to  $9.0 \times 10^6$  7 GeV pulses and the endplates are examined ultrasonically about every  $1.5 \times 10^6$  pulses.

A number of investigations are still proceeding to obtain further information concerning the behaviour of the rotor.

The interplay of all the forces acting on the rotor is very complex and the mechanism of fretting fatigue is not perfectly understood. On any keyed form of pole construction relative movement must occur within such keyed assemblies. It was therefore considered prudent to order a spare rotor having solid poles forged integrally with the body, although it is realised that in this form of construction problems can arise in the pole shoe to pole body assembly regions.

The possibility of replacing the complete rotating plant by a saturable reactor network compensation device which would enable 7 GeV pulsing direct from the electricity supply network is also being considered.

8.0 Acknowledgements

The work described in this paper was the result of a sustained combined effort on the part of a large number of people at the Rutherford High Energy Laboratory, the English Electric Co., Ltd., and Lloyds Register of Shipping. The authors would particularly stress the extent of their colleagues' contribution and find it difficult to single out names.

Nevertheless they feel they must specifically acknowledge the contributions made by Dr. H. H. Atkinson and Mr. A. J. Middleton of R.H.E.L. and Messrs. I. E. McShane and P. G. Morton of E.E. Co.

The authors also wish to acknowledge the permission given by their respective organisations to publish this paper.

References

1. BOWLES, P., et al., "Magnet Power Supply for the 7 GeV Proton Synchrotron Nimrod." PROCEEDINGS I.E.E., VOL 110, No. 3, March 1963, p.p. 561-602.
2. COYLE, M. B., WATSON, S. J., "Fatigue Strength of Turbine Shafts with Shrunk-on Discs." PROCEEDINGS I. MECH. E., 1963-4, pp 147-179.
3. ATKINSON, H. H., et al., "Photoelastic Investigation of Stress in Nimrod Alternator Pole End Plates." (In course of preparation at the Rutherford High Energy Laboratory.)

Table 1 Estimated endplate stresses

Stress Components	Mean Tensile Direct	Tensile Transverse Bending	Tensile Longitudinal Bending #	Design
Due to lamination clamping pressure			-1700 to -3400	OLD
Centrifugal (950r/min)	+24000		+1200 to +17900	Mean stress is therefore 39600 max to
Due to speed change(PRF approx. 0.5c/s at 7GeV)	± 1000		± 470 to ± 760	31200 min
Due to gravitational effect (approx. 16 c/s)	± 30	± 390	± 1300 to ± 1800	Alternating stress is ± 4240 max to
Due to load torque(PRF approx. 0.5c/s at 7GeV)		± 1200		± 3450 min
Due to shaft torsional oscillation (approx. 20-4c/s)		± 1000		
Due to lamination clamping pressure			-2700 to -4000	NEW
Centrifugal (950r/min)	+24000		+ 5600 to +17000	Mean stress is therefore 31650 max to
Due to speed change(PRF approx. 0.5c/s at 7GeV)	± 1000		± 220 to ± 470	24950 min
Due to gravitational effect (approx. 16 c/s)	± 30	± 400	± 670 to ± 900	Alternating stress is ± 3130 max to
Due to load torque(PRF approx. 0.5c/s at 7GeV)		± 1300		± 2680 min
Due to shaft torsional oscillation (approx. 20-4c/s)		± 1100		

Key  
 ± Alternating stresses  
 - Compressive stresses  
 + Tensile stresses

Note #  
 Estimates for longitudinal bending stresses have a wide range dependent upon assumptions made concerning support given by laminations, friction dovetail fixing characteristics etc.

All figures in lb/in<sup>2</sup> & not inclusive of stress concentration factors. The figures are for 7GeV operation with a speed variation of 40r/min.

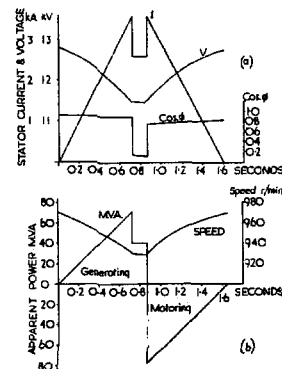


Fig. 1 Simplified characteristics showing alternator loading during a typical pulse

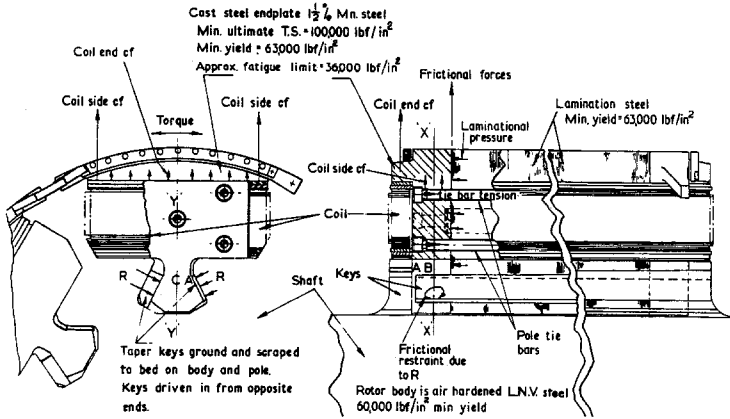


Fig. 2 Original pole construction

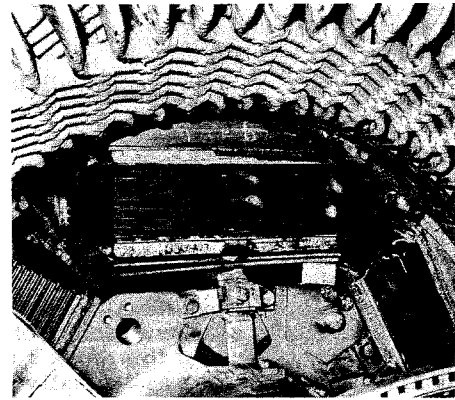


Fig. 3 Damaged pole and stator

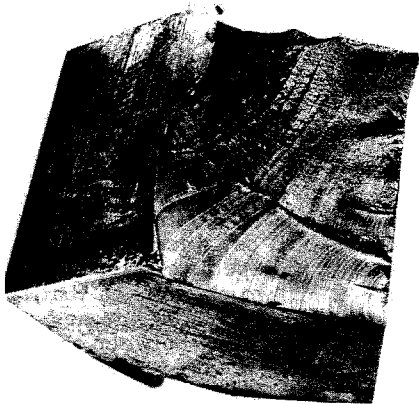


Fig. 4 Lower half of fractured dovetail

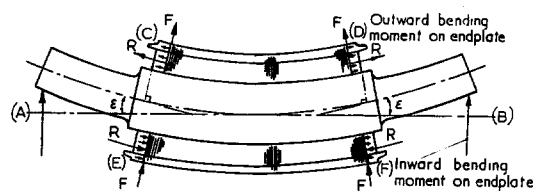


Fig. 5 Shaft stress catenary effect

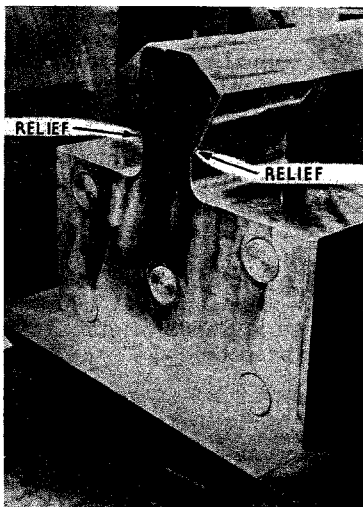


Fig. 6 Part of re-designed endplate pole assembly showing reliefs

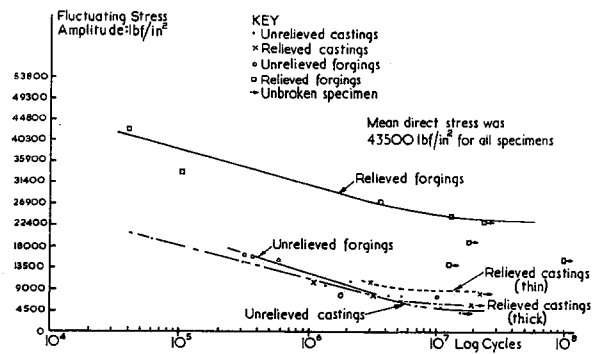


Fig. 7 Fatigue curves obtained from test rig results